3-2013

Three-Dimensional Engineered Matrix to Study Cancer Stem Cells and Tumorsphere Formation: Effect of Matrix Modulus

Xiaoming Yang
University of South Carolina - Columbia, yang42@mailbox.sc.edu

Samaneh Kamali Sarvestani
University of South Carolina, sarvests@email.sc.edu

Seyedsina Moeinzadeh
University of South Carolina - Columbia, sinamoeinzadeh@sc.edu

Xuezhong He

Esmaiel Jabbari
University of South Carolina - Columbia, jabbari@mailbox.sc.edu

Publication Info

Published in *Tissue Engineering Part A*, Volume 19, Issue 5-6, 2013, pages 669-684.

Yang, X., Sarvestani, S. K., Moeinzadeh, S., He, X., & Jabbari, E. Three-Dimensional Engineered Matrix to Study Cancer Stem Cells and Tumorsphere Formation: Effect of Matrix Modulus. *Tissue Engineering Part A 19*(5-6), 669-684.
http://dx.doi.org/10.1089/ten.tea.2012.0333

TISSUE ENGINEERING: Part A
Volume 19, Numbers 5 and 6, 2013

DOI: 10.1089/ten.tea.2012.0333

Three-Dimensional-Engineered Matrix to Study Cancer Stem Cells and Tumorsphere Formation: Effect of Matrix Modulus

Xiaoming Yang, PhD,[1,2,*] Samaneh K. Sarvestani, BS,[1,*] Seyedsina Moeinzadeh, BS,[1] Xuezhong He, PhD,[1] and Esmaiel Jabbari, PhD[1]

Maintenance of cancer stem cells (CSCs) is regulated by the tumor microenvironment. Synthetic hydrogels provide the flexibility to design three-dimensional (3D) matrices to isolate and study individual factors in the tumor microenvironment. The objective of this work was to investigate the effect of matrix modulus on tumorsphere formation by breast cancer cells and maintenance of CSCs in an inert microenvironment without the interference of other factors. In that regard, 4T1 mouse breast cancer cells were encapsulated in inert polyethylene glycol diacrylate hydrogels and the effect of matrix modulus on tumorsphere formation and expression of CSC markers was investigated. The gel modulus had a strong effect on tumorsphere formation and the effect was bimodal. Tumorsphere formation and expression of CSC markers peaked after 8 days of culture. At day 8, as the matrix modulus was increased from 2.5 kPa to 5.3, 26.1, and 47.1 kPa, the average tumorsphere size changed from 37 ± 6 μm to 57 ± 6, 20 ± 4, and 12 ± 2 μm, respectively; cell number density in the gel changed from $0.8 \pm 0.1 \times 10^5$ cells/mL to $1.7 \pm 0.2 \times 10^5$, $0.4 \pm 0.1 \times 10^5$, and $0.2 \pm 0.1 \times 10^5$ cells/mL after initial encapsulation of 0.14×10^5 cells/mL; and the expression of CD44 breast CSC marker changed from 17 ± 4-fold to 38 ± 9-, 3 ± 1-, and 2 ± 1-fold increase compared with the initial level. Similar results were obtained with MCF7 human breast carcinoma cells. Mouse 4T1 and human MCF7 cells encapsulated in the gel with 5.3 kPa modulus formed the largest tumorspheres and highest density of tumorspheres, and had highest expression of breast CSC markers CD44 and ABCG2. The inert polyethylene glycol hydrogel can be used as a model-engineered 3D matrix to study the role of individual factors in the tumor microenvironment on tumorigenesis and maintenance of CSCs without the interference of other factors.

Introduction

Breast cancer is the most common cancer among women in industrialized countries. The development of breast cancer is a multiple-step process and regulated by the tumor microenvironment.[1] This process may take many years and is difficult to follow *in vivo*. Therefore, there is a need to develop *in vitro* models to study the molecular basis of tumorigenesis and progression. Most *in vitro* studies use standard two-dimensional (2D) cell culture. However, cells grown on 2D tissue culture behave differently from those grown in physiological 3D environment due to the lack of proper cell–cell and cell–matrix interactions as well as the gradient of nutrients and growth factors, which are known to play critical roles in cancer initiation, progression, and metastasis.[2] For example, when cancer cells are cultured in 2D plates, their malignancy is reduced compared with those under *in vivo* conditions.[3] Animal models are also frequently used to study molecular pathways and drug response in cancer research. In these cases, either animal tumors grown in syngeneic animals or human tumors grown in immunocompromised animals are used. Therefore, animal models may not adequately reproduce the features of human cancers *in vivo*.

To bridge the gap between the 2D cell culture system and the *in vivo* system, the 3D *in vitro* cell culture system has emerged as another approach for cancer research. In many 3D models, cell lines or cells from dissociated tissues are embedded in 3D matrices and cultured to promote cell–cell interaction, adhesion, migration, and *in vivo*–like morphogenesis. Comparison between 2D and 3D cultures has revealed significant differences in all aspects of cell behavior, that is, from cell shape

[1]Biomimetic Materials and Tissue Engineering Laboratory, Department of Chemical Engineering, University of South Carolina, Columbia, South Carolina.
[2]Dorn Research Institute, Columbia, South Carolina.
*These two authors contributed equally to this article.

and growth to gene expression and response to stimuli.[4] Various types of materials have been used to generate a 3D matrix. Type 1 collagen and Matrigel™ are the most widely used matrices[5] because they are biocompatible and support adhesion and growth of many cell types.[6,7]

Alginate and agarose gels are also used as a matrix to study the behavior of breast cancer cells under a 3D condition.[8,9] However, it is difficult to isolate and study cell response to individual factors in the microenvironment with naturally derived matrices that have many interactions with cell surface receptors.[10]

In that regard, synthetic gels provide enormous flexibility in designing 3D matrices with a wide range of mechanical, physical, and biological properties that are crucial to the maintenance, differentiation, maturation, and fate of the encapsulated cells.[11–13] Among them, polyethylene glycol (PEG) hydrogel, due to its inert nature, has been used extensively as an engineered matrix for cell encapsulation to elucidate the effect of factors in the microenvironment on cell fate.[14–17] Among the factors in the microenvironment, matrix stiffness or elastic modulus plays an important role in regulating cell function in 2D as well as 3D culture systems.[18] In 3D culture systems, elastic modulus of the matrix can direct differentiation of encapsulated stem cells and shift the balance of cell proliferation and apoptosis.[19–21] *In vivo*, cells have the ability to sense and respond to matrix stiffness by synthesizing the appropriate extracellular matrix (ECM) composition as the mechanical properties and composition of hard and soft tissues differ significantly. Cells need to respond appropriately to the environmental cues for survival.[22] Likewise, the proliferation, differentiation, migration, and apoptosis of cancerous cells in the tumor tissue are regulated by matrix stiffness.[23–25]

Although the effect of matrix stiffness on the response of normal stem cells has been studied extensively,[26–29] the effect on cancer stem cells (CSCs) encapsulated within an inert microenvironment has not been investigated. Normal stem cells and CSCs use similar signaling pathways to maintain their stemness. However, they may respond to the environmental cue differently. The microenvironment or niche under normal conditions inhibits stem cell proliferation and differentiation. However, CSCs, due to mutations in the cell, are self-sufficient with respect to proliferation.[30,31] It has been proposed that the stem cell niche is converted from proliferation inhibitory to signals favoring cell proliferation in the case of CSCs.[32]

The objective of this work was to investigate the effect of matrix elastic modulus on the formation, growth, and maintenance of CSCs by tumor cells encapsulated in PEG hydrogels, in the absence of attached ligands that interact with cell surface receptors. We show that the formation and maintenance of 4T1 mouse breast cancer cells and MCF7 human breast cancer cells are modulated by the elastic modulus of the PEG matrix. This inert engineered 3D matrix provides a novel tool to control and investigate the effect of microenvironmental factors on maintenance of CSCs *in vitro*.

Materials and Methods

Materials

PEG (nominal molecular weight 4.6 kDa), dichloromethane (DCM), N,N-dimethylformamide, diethyl ether, and hexane were purchased from Acros (Fairfield, OH). Calcium hydride, triethylamine (TEA), paraformaldehyde, 4,6-diamidino-2-phenylindole (DAPI), insulin, penicillin, and streptomycin were purchased from Sigma-Aldrich (St. Louis, MO). Basic fibroblast growth factor (bFGF) and epidermal growth factor (EGF) were purchased from Lonza (Allendale, NJ). Bovine serum albumin (BSA) was obtained from Jackson ImmunoResearch (West Grove, PA). Dulbecco's phosphate-buffered saline (PBS), trypsin–ethylenediaminetetraacetic acid, RPMI-160 cell culture medium, Dulbecco's modified Eagle's medium (DMEM)–F12 medium, fetal bovine serum (FBS), Alexa Fluor® 594 Phalloidin, and Quant-it PicoGreen double-stranded DNA (dsDNA) reagent kit were purchased from Invitrogen (Carlsbad, CA). Horse serum was purchased from PAA Laboratories (Etobicoke, Ontario) and DMEM-F12 was from Mediatech (Manassas, VA). Spectro/Por dialysis tube (molecular weight cutoff 3.5 kDa) was purchased from Spectrum Laboratories (Rancho Dominquez, CA). DCM was purified by distillation over calcium hydride. All other solvents were reagent grade and were used as received without further purification. Anti-CD44 antibody (HCAM, DF1485) was from Santa Cruz Biotechnology (Santa Cruz, CA). Monoclonal anti-bromodeoxyuridine (anti-BrdU) antibody proliferation marker (produced in mouse) was obtained from Sigma-Aldrich. Fluorescent conjugated secondary antibodies were obtained from Invitrogen. 4T1 mouse breast carcinoma and MCF7 human breast adenocarcinoma cell lines were received from the Scripps Research Institute (La Jolla, CA) and American Type Culture Collection (Manassas, VA), respectively. The live/dead calcein AM (cAM) and ethidium homodimer-1 (EthD) cell viability/cytotoxicity kit was purchased from Molecular Probes (Life Technologies, Grand Island, NY).

Macromer synthesis and characterization

The PEG macromer was functionalized with acrylate groups to produce polyethylene glycol diacrylate (PEGDA) by the reaction of acryloyl chloride with hydroxyl end groups of PEG, as shown in Figure 1A. TEA was used as the reaction catalyst. Prior to the reaction, PEG was dried by azeotropic distillation from toluene to remove residual moisture. The polymer was dissolved in dried DCM in a reaction flask; the flask was immersed in an ice bath to cool the polymer solution and limit the temperature rise from the exothermic reaction. In a typical reaction, 5.6 mL acryloyl chloride and 9.7 mL TEA, each dissolved in DCM, were added drop-wise to the reaction with stirring. The reaction was allowed to proceed for 12 h under nitrogen flow. After completion of the reaction, the solvent was removed by rotary evaporation and the residue was dissolved in anhydrous ethyl acetate to precipitate the by-product triethylamine hydrochloride salt. Next, ethyl acetate was removed by vacuum distillation; the macromer was re-dissolved in DCM and precipitated twice in ice-cold ethyl ether. The macromer was dissolved in dimethylsulfoxide and dialyzed against distilled deionized water to remove the by-products. The PEGDA product was freeze-dried and stored at −20°C. The chemical structure of the functionalized macromer was characterized by a Varian Mercury-300 proton nuclear magnetic resonance (^{1}H-NMR) (Varian, Palo Alto, CA) at ambient conditions with a resolution of 0.17 Hz. The sample was dissolved in deuterated chloroform at a concentration of 5 mg/mL and 1% v/v tetramethylsilane (TMS) was used as the internal standard.

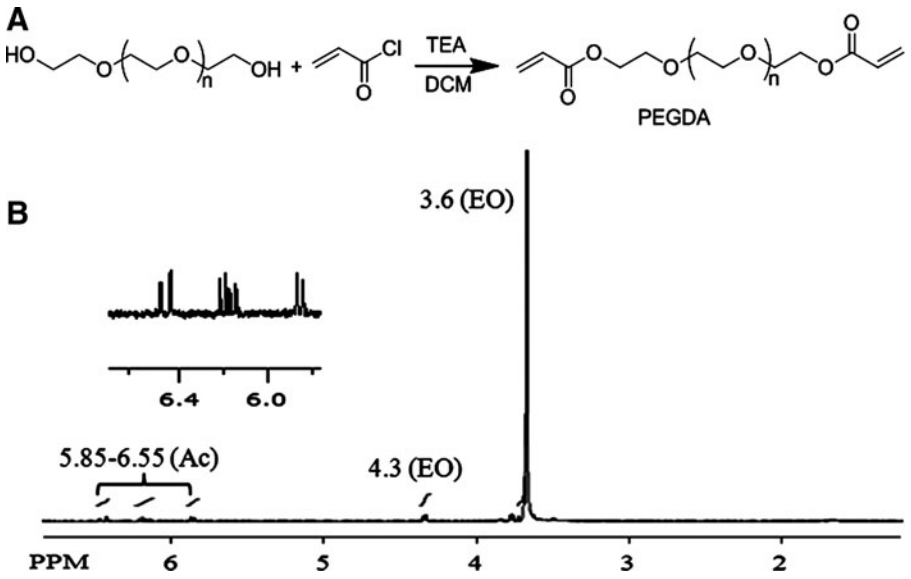

FIG. 1. **(A)** Reaction scheme for acrylation of PEG macromer and **(B)** ^{1}H-NMR spectrum of PEGDA macromer. The chemical shifts between 5.85 and 6.55 ppm due to acrylate hydrogens are enlarged in the inset of the NMR spectrum. PEG, polyethylene glycol; PEGDA, polyethylene glycol diacrylate; NMR, nuclear magnetic resonance.

Hydrogel synthesis and measurement of gel modulus

The PEGDA macromers were crosslinked in aqueous solution by ultraviolet (UV)-initiated radical polymerization with 4-(2-hydroxyethoxy)phenyl-(2-hydroxy-2-propyl) ketone (Irgacure 2959; CIBA, Tarrytown, NY) photoinitiator. Five milligrams of initiator was dissolved in 1 mL PBS at 50°C. The macromer was dissolved in PBS by vortexing and heating to 50°C. To prepare 7.5%, 10%, 15%, 20%, and 25% PEGDA hydrogel precursor solutions, 22.5, 30, 45, 60, and 75 mg of PEGDA macromer were mixed with 278, 270, 255, 240, and 225 μL of the initiator solution, respectively, by vortexing for 5 min. For cell loading, 1.4×10^5/mL 4T1 cells suspended in PBS were added to the macromer solution and mixed gently with a glass rod. The hydrogel precursor solutions were degassed and transferred to a polytetrafluoroethylene (PTFE) mold (5 cm × 3 cm × 750 μm), covered with a transparent glass plate, fastened with clips, and UV irradiated with a BLAK-RAY 100 W mercury, long-wavelength (365 nm) UV lamp (Model B100-AP; UVP, Upland, CA) for 10 min. Disk-shaped samples were cut from the gel using an 8-mm cork borer and swollen in PBS for 24 h at 37°C. To measure the gel's elastic modulus, samples were loaded on the Peltier plate of the rheometer (TA Instruments, New Castle, DE) and subjected to a uniaxial compressive force at a displacement rate of 7.5 μm/s. The slope of the linear fit to the stress–strain curve for 5%–10% strain was taken as the elastic modulus (E) of the gels.

CSC culture and characterization

4T1 and MCF7 tumor cells were cultured in RPMI-1640 medium with 10% FBS under 5% CO_2 at 37°C. Cells were trypsinized after reaching 70% confluency. PEGDA macromer was dissolved in PBS and sterilized by filtration with a 0.2 μm filter. Next, 1.4×10^5/mL 4T1 or MCF7 cells suspended in PBS were added to the macromer solution with final PEGDA concentrations ranging 5–25 wt%, and mixed gently with a pre-sterilized glass rod. The cell-suspended hydrogel precursor solution was crosslinked with UV for 10 min. After crosslinking, the gel was cut into disks and incubated in stem cell culture medium in ultra-low-attachment tissue culture plates under 5% CO_2. The stem cell medium consisted of DMEM-F12 supplemented with 0.4% BSA, 5 μg/mL insulin, 40 ng/mL bFGF, 20 ng/mL EGF, 5% horse serum, 100 U/mL penicillin, and 100 μg/mL streptomycin.[33] For growing tumorspheres in suspension, trypsinized 4T1 cells were cultured on ultra-low-attachment tissue culture plates with stem cell culture medium under 5% CO_2 at 37°C as described previously.[33–35] The gold standard for characterization of CSC tumorspheres for stemness is by the ability to form tumor *in vivo*.[36,37] To test for tumor formation, a stable 4T1 cell line that expressed luciferase (4T1-Luc) was established as described.[38] Luciferase expression vector pGL4.50[Luc2/CMV/Hygro] (Promega, Madison, WI) was transfected into 4T1 cells by Lipofectamine 2000 (Invitrogen), according to the manufacturer's instructions, to generate a cell line expressing luciferase as a reporter.[38] After 24 h, cells were trypsinized and cultured in RPMI-1640 medium with 400 μg/mL of hygromycin for 3 weeks to generate 4T1-Luc cells. 4T1-Luc cells were cultured on adhesion plates with regular RPMI-1640 culture medium or on ultra-low-attachment plates with stem cell culture medium as described previously. After one week, cells were trypsinized and counted. Different number of cells (5000 and 50,000 cells from adhesion plates or 500, 1000, and 5000 tumorsphere cells from ultra-low-attachment plates) was injected subcutaneously in syngeneic Balb/c mice (6 mice/group). One week after inoculation, 100 μL of D-Luciferin (30 mg/mL; Caliper, Hopkinton, MA) was injected subcutaneously and mice were imaged 10 min after Luciferin injection by Caliper's IVIS Spectrum imaging system (Caliper Life Sciences, Hopkinton, MA).

Cell imaging and determination of cell number

To determine cell viability, gels were stained with cAM/EthD live/dead dyes 2 days after encapsulation to image live and dead cells, respectively. Stained samples were imaged with an inverted fluorescent microscope (Nikon Eclipse Ti-ε; Nikon, Melville, NY). Cell viability was quantified by dividing the image into smaller squares and counting the

number of live and dead cells. At each time point, the gel samples were removed from the culture media and stained for imaging. Samples were rinsed twice with PBS and fixed with 4% paraformaldehyde for 3 h. After fixation, cells were permeabilized using PBS containing 0.1% Triton X-100 for 5 min. After rinsing, cells were incubated with Alexa 488 phalloidin (1:200 dilution) and DAPI (1:5000 dilution) to stain actin filaments of the cell cytoskeleton and cell nuclei, respectively. Stained samples were imaged with a Nikon Eclipse Ti-ε inverted fluorescent microscope. For visualization of cell uniformity, a confocal fluorescent microscope (Zeiss LSM-510 META Axiovert; Carl Zeiss, Germany) was used to obtain 2D images (90-μm-thick layers) of the stained gels in the direction of thickness, as described.[39] For determination of cell number, the gel samples were homogenized, cells were lysed, and aliquots were used to measure the dsDNA content using a Quant-it PicoGreen assay as described.[40] Briefly, an aliquot (100 μL) of the working solution was added to 100 μL of the cell lysate and incubated for 4 min at ambient conditions. The fluorescence of the solution was measured with a plate reader (Synergy HT; Bio-Tek, Winooski, VT) at emission and excitation wavelengths of 485 and 528 nm, respectively. Measured fluorescent intensities were correlated to cell numbers using a calibration curve constructed with 4T1 or MCF7 cells of known concentration ranging from zero to 10^5 cells/mL.

BrdU retention assay and immunofluorescent imaging

BrdU label retention was used to identify mammary CSCs as described.[41,42] Nonconfluent 4T1 cells were incubated with 10 μM of BrdU for 10 days to label the DNA by incorporating BrdU into replicating DNA in place of thymidine. Next, the BrdU-labeled cells were encapsulated in the gel and incubated in stem cell culture medium to form tumorspheres as described previously. At each time point, the retention of BrdU in the encapsulated cells was imaged by immunofluorescent staining with anti-BrdU antibodies as described.[41] At each time point, tumorspheres encapsulated in the gel samples were processed and stained for immunofluorescent imaging of BrdU-labeled cells or CD44 marker as described.[43] Gel samples were fixed and permeabilized for 3 h at 4°C in PBS containing 4% paraformaldehyde and 1% Triton X-100, followed by rinsing with PBS (3 × 10 min). Tumor spheroids were then dehydrated in an ascending series of methanol at 4°C in PBS (25%, 50%, 75%, and 95% for 30 min each and 100% for 5 h) and rehydrated in the same descending series and washed in PBS (3 × 10 min). Next, samples were blocked with PBS containing 0.1% Triton X-100 (PBST) and 3% BSA overnight at 4°C and washed with PBS (2 × 15 min). Then, samples were incubated with primary antibodies (anti-CD44 antibody or anti-BrdU antibody) diluted in PBST on a gently rocking rotator at 4°C overnight followed by rinsing with PBST (4 × 30 min). Samples were then incubated with Alexa Fluor–conjugated secondary antibodies for 2 h and rinsed with PBST (4 × 10 min). The cell nuclei were counterstained with DAPI (1:5000 dilution in PBS) and imaged with a Nikon Eclipse Ti-ε inverted fluorescent microscope.

mRNA analysis

Total cellular RNA of the gel samples was isolated using TRIzol (Invitrogen) as described.[40] About 250 ng of the extracted purified RNA was reverse transcribed to cDNA by SuperScript II Reverse Transcriptase (Invitrogen) with the random primers. The obtained cDNA was subjected to real-time quantitative polymerase chain reaction (RT-qPCR) amplification with appropriate gene-specific primers. RT-qPCR was performed to analyze the differential expression of CSC markers *CD44* (4T1 and MCF7), *CD24* (4T1), *ABCG2* (4T1 and MCF7), and *SCA1* (4T1) genes with SYBR green RealMasterMix (Eppendorf, Hamburg, Germany) using Bio-Rad iCycler PCR system (Bio-Rad, Hercules, CA). The expression level of *GAPDH* gene was used as an internal control. The primers for RT-PCR were designed by Primer 3 software (http://frodo.wi.mit.edu). The following forward and reverse primers synthesized by Integrated DNA Technologies (Coralville, IA) were used: *mouse GAPDH*: forward 5′-CAT GGC CTT CCG TGT TCC TA-3′ and reverse 5′-CCT GCT TCA CCA CCT TCT TGA-3′; *mouse CD44*: forward 5′-GAA TGT AAC CTG CCG CTA CG-3′ and reverse 5′-GGA GGT GTT GGA CGT GAC-3′; *mouse CD24*: forward 5′-CTT CTG GCA CTG CTC CTA CC-3′ and reverse 5′-GAG AGA GAG CCA GGA GAC CA-3′; *mouse ABCG2*: forward 5′-AGC AGC AAG GAA AGA TCC AA-3′ and reverse 5′-GGA ATA CCG AGG CTG ATG AA-3′; *mouse SCA1*: forward 5′-TGG ACA CTT CTC ACA CTA-3′ and reverse 5′-CAG AGC AAG AGG GTC TGC AGG AG-3′; *human GAPDH*: forward 5′-GAG TCA ACG GAT TTG GTC GT-3′ and reverse 5′-TTG ATT TTG GAG GGA TCT CG-3′; *human CD44*: forward 5′-GGC TTT CAA TAG CAC CTT GC-3′ and reverse 5′-ACA CCC CTG TGT TGT TTG CT-3′; and *human ABCG2*: forward 5′-CAC CTT ATT GGC CTC AGG AA-3′ and reverse 5′-CCT GCT TGG AAG GCT CTA TG-3′. The relative gene expression levels were quantified by the 2–ΔΔCT method as described.[44,45] The relative gene expression was expressed as fold difference compared with that at time zero.

Statistical analysis

Data are expressed as mean ± standard deviation. All experiments were done in triplicate. Significant differences between groups were evaluated using a two-way analysis of variance (ANOVA) with replication test followed by a two-tailed Student's *t*-test. A value of $p < 0.05$ was considered statistically significant.

Results

Macromer characterization and hydrogel modulus

The reaction scheme for acrylation of PEG macromer and the NMR spectrum of PEGDA are shown in Figure 1A and 1B, respectively. The chemical shifts with peak positions at 3.6 and 4.3 ppm were attributed to the methylene hydrogens ($=CH_2$) of PEG attached to ether ($-CH_2-O-CH_2-$) and ester ($-CH_2-OOC-$) groups, respectively. The shifts with peak positions from 5.85 to 6.55 ppm (see inset in Fig. 1B) were attributed to the vinyl hydrogens ($-CH=CH_2$) of the acrylate group at the end of each macromer arm as follows: peak positions in the 5.82–5.87 ppm range were associated with the trans proton of unsubstituted carbon of the Ac; those in the 6.10–6.20 ppm range corresponded to the protons bonded to monosubstituted carbon of the Ac; and those in the 6.40–6.46 ppm range were associated with the proton of unsubstituted carbon of the acrylate group. The number of acrylate groups per macromer was determined from the ratio

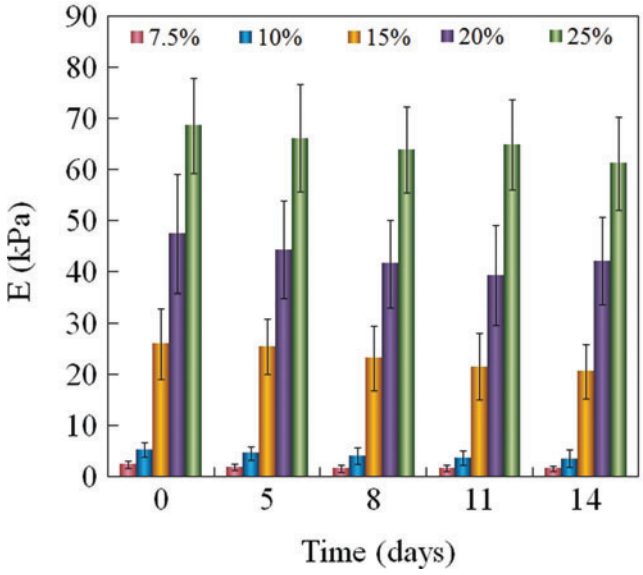

FIG. 2. Effect of macromer concentration on elastic modulus of 4T1-cell-loaded (1.4×10^5 cells/mL) PEGDA hydrogels with incubation time. Error bars correspond to mean ± 1 SD for $n=3$. Color images available online at www.liebertpub.com/tea

of NMR shifts between 5.85 and 6.55 ppm (acrylate hydrogens) to those at 3.6 and 4.2 ppm (PEG hydrogens).[46,47] Based on NMR results, the average degree of acrylation was 89% and there was on average 1.8 ± 0.1 acrylates in the PEGDA macromer. Disk-shaped hydrogels with 8-mm diameter and 750-μm thickness were fabricated for determination of elastic modulus and cell encapsulation. The effect of macromer concentration and incubation time on the elastic modulus of PEGDA hydrogel, loaded with 4T1 cells, is shown in Figure 2. Macromer concentration in the precursor solution affected the elastic modulus of the hydrogel. The elastic modulus increased from 2.5 ± 0.7 kPa to 5.3 ± 1.4, 26.1 ± 6.9, 47.5 ± 11.6, and 68.6 ± 9.3 kPa as the macromer concentration was increased from 5% to 10%, 15%, 20%, and 25%, respectively. The elastic modulus of the gels, with encapsulated 4T1 cells, did not change significantly during 14 days of incubation in the cell culture medium, as shown in Figure 2.

Tumorsphere characterization

Tumorsphere formation on ultra-low-attachment plates is a commonly used method to enrich CSCs *in vitro*, while the gold standard for characterization of CSC tumorspheres is by the ability to form tumor *in vivo*.[36,37] 4T1-Luc cells were cultured on regular adhesion plates or ultra-low-attachment plates. After one week, cells in monolayers (adhesion plates) and in spheres (ultra-low-attachment plates) were collected and subcutaneously inoculated in syngeneic Balb/c mice. Tumor formation in mice was determined by imaging the expression of luciferase one week after inoculation. Figure 3 compares tumor formation by cells on adhesion plates (Fig. 3A) and cells from tumorspheres on ultra-low-attachment plates (Fig. 3B). The left and right images in Figure 3A are for 5000 and 50,000 4T1-Luc cells on adhesion plates. The left, center, and right images in Figure 3B are for 500, 1000, and 5000 4T1-Luc cells from tumorspheres on ultra-low-

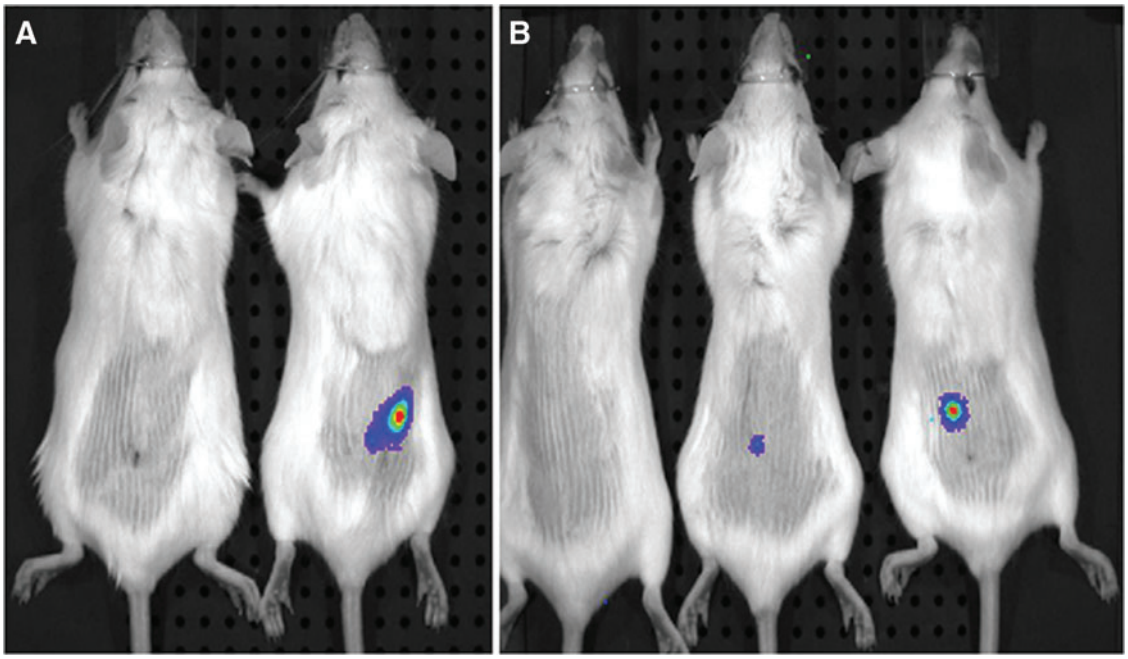

FIG. 3. Comparing *in vivo* tumor formation of 4T1 cells from adhesion plates **(A)** with 4T1 cells from tumorspheres on ultra-low-attachment plates **(B)**. The left and right images in **(A)** show tumor formation by inoculation of 5000 and 50,000 4T1-Luc cells, respectively. The left, center, and right images in **(B)** show tumor formation by inoculation of 500, 1000, and 5000 4T1-Luc cells from tumorspheres. 4T1-Luc cells were inoculated subcutaneously in Balb/c mice. After one week, the expression of luciferase in tumors was imaged. The light blue, dark blue, and red color images correspond to low, medium, and high luciferase intensity, proportional to the size of the tumor formed. Color images available online at www.liebertpub.com/tea

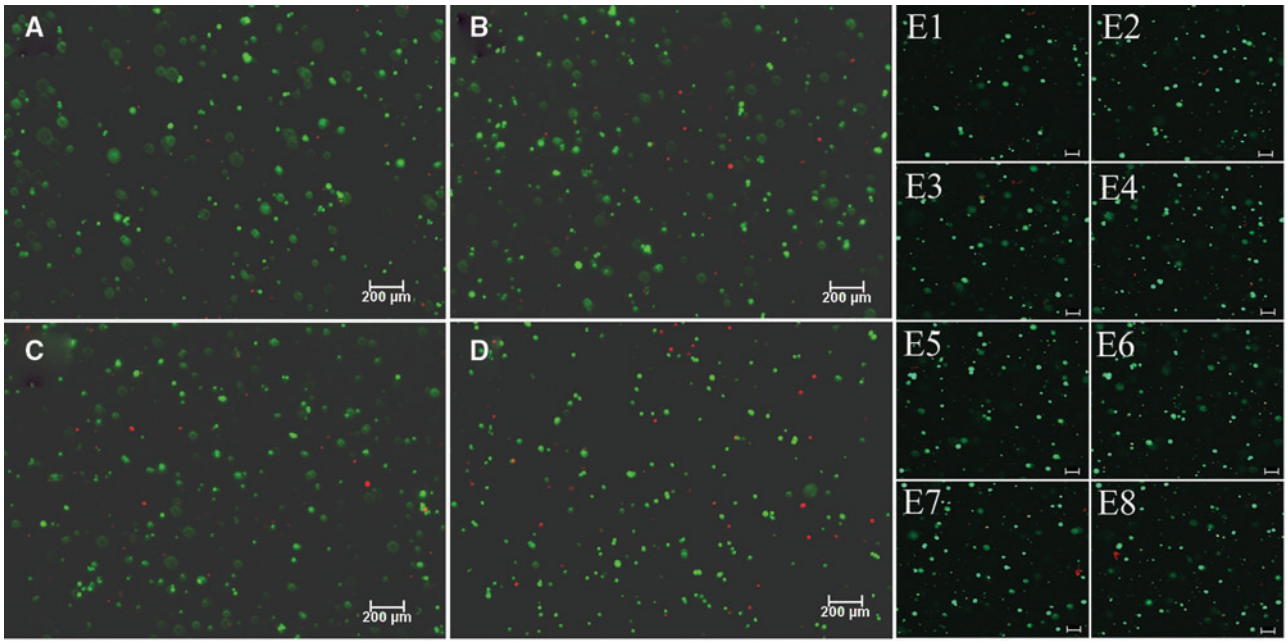

FIG. 4. Live (green) and dead (red) image of 4T1 cells 2 days after encapsulation in PEGDA hydrogels with moduli of **(A)** 2.5 kPa, **(B)** 5.3 kPa, **(C)** 26.1 kPa, and **(D)** 47.5 kPa. The scale bar in images **(A–D)** is 200 μm. Based on image analysis, the percent viable cells for 2.5, 5.3, 26.1, 47.5, and 68.6 kPa gels was 94 ± 4, 91 ± 3, 92 ± 3, 90 ± 4, and 89 ± 4, respectively. Images **(E1–E8)** on the right show the uniformity of cell seeding and cell viability in successive 90 μm layers in the direction of thickness for 5.3 kPa gel, obtained with a confocal fluorescent microscope. The scale bar in images **(E1–E8)** is 200 μm. Color images available online at www.liebertpub.com/tea

attachment plates. According to the images in Figure 3, 1000 tumorsphere cells were sufficient to form a tumor *in vivo* while it required 50,000 regular tumor cells to form a tumor. These results demonstrate that tumorspheres formed by 4T1 cells *in vitro* had enriched CSC subpopulation.

Tumorsphere formation in hydrogel

4T1 tumor cells were encapsulated in PEGDA hydrogels with elastic moduli ranging from 2 to 70 kPa and cultured in stem cell medium for 2 weeks. Images of live and dead cells 2 days after encapsulation in PEGDA gels with moduli of 2.5, 5.3, 26.1, and 47.5 kPa are shown in Figure 4A through 4D, respectively. Based on image analysis, the percent viable cells for 2.5, 5.3, 26.1, 47.5, and 68.6 kPa gels were 94 ± 4, 91 ± 3, 92 ± 3, 90 ± 4, and 89 ± 4, respectively. These results show that the gel modulus did not have a significant effect on viability of 4T1 cells after encapsulation. To determine cell uniformity and viability, a confocal microscope was used to image cells in the direction of thickness and the results are shown in Figure 4E1–E8. Images in Figure 4E show uniform cell seeding and cell viability within the gel in the thickness direction.

Fluorescent images in Figure 5 show the extent of cell aggregation and spheroid formation with incubation time for 4T1 gels with modulus of 2.5 kPa (Fig. 5, column 1), 5.3 kPa (Fig. 5, column 2), 47.5 kPa (Fig. 5, column 3), and MCF7 gel with 5.3 kPa (Fig. 5, column 4). Rows 1, 2, 3, and 4 in Figure 5 correspond to incubation times of 5, 8, 11, and 14 days, respectively. Spheroid formation was observed in soft gels with moduli of 2.5 and 5.3 kPa as early as day 5 (columns 1, 2, and 4 in Fig. 5) while cells in the more stiff gels with modulus of 47.5 kPa and higher remained as single cells or small cell aggregates (< 25 μm). MCF7 human breast cancer cells also formed spheres when encapsulated in the gel with modulus of 5.3 kPa (Fig. 5, column 4). At any time point, size of the tumorspheres in the 5.3 kPa gel was higher than that of 2.5 kPa gel. Lower magnification images showing the number density of 4T1 (Fig. 6, column 1) and MCF7 (Fig. 6, column 2) tumorspheres in PEGDA gels with elastic moduli of 2.5 kPa (Fig. 6, row 1), 5.3 kPa (Fig. 6, row 2), 26.1 kPa (Fig. 6, row 3), and 47.5 kPa (Fig. 6, row 4) after 8 days of incubation are shown in Figure 6, respectively. According to Figure 6, the tumorsphere size and number density initially increased with increasing matrix modulus from 2.5 to 5.3 kPa and then decreased when modulus was increased to 26.1 and 47.5 kPa. Tumorspheres with diameter > 100 μm were observed only in the gels with modulus of 2.5 and 5.3 kPa but the fraction of large tumorspheres (> 100 μm) was significantly higher in the 5.3 kPa gel. It should be noted that the size of MCF7 spheroids in the gels was less than that of 4T1.

Tumorsphere size and number density

The effect of hydrogel modulus on average tumorsphere diameter and size distribution with incubation time is shown in Figure 7A and 7B for 4T1 cells and Figure 7D and 7E for MCF7 cells, respectively. The average 4T1 tumorsphere diameter increased from 10 μm at day zero to 80, 140, 30, 15, and 10 μm after 14 days as the gel modulus increased from 2.5 kPa to 5.3, 26.1, 47.5, and 68.6 kPa, respectively, while tumorsphere diameter for MCF7 cells increased from 8 μm at day zero to 60, 90, 29, 13, and 11 μm after 14 days. For 4T1 cells in the softest gel (2.5 kPa modulus), 25% of the cell aggregates at day 8 had < 20 μm size (single-cell fraction) while there was no single-cell subpopulation in the gel with 5.3 kPa modulus. For MCF7 cells after 8 days, 28% and 3% of the cell

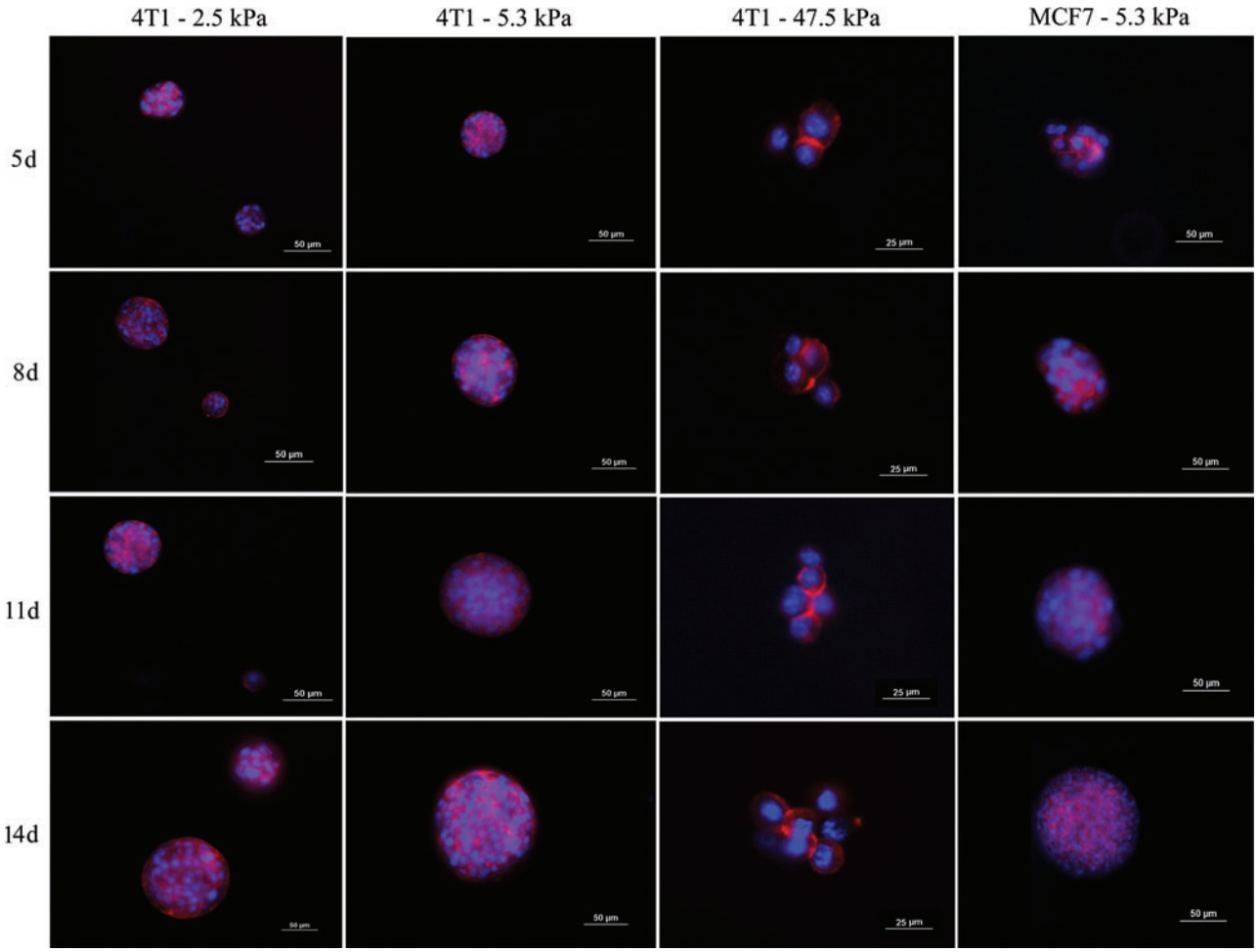

FIG. 5. Evolution of tumorsphere formation by 4T1 tumor cells encapsulated in PEGDA hydrogels with elastic modulus of 2.5 kPa (left column), 5.3 kPa (center left column), and 47.5 kPa (center right column), and MCF7 tumor cells encapsulated in the 5.3 kPa gel (left column) as a function of incubation time. Rows 1, 2, 3, and 4 correspond to incubation times of 5, 8, 11, and 14 days, respectively. At each time point, encapsulated cells were stained with phalloidin for cytoskeleton (red) and DAPI for nucleus (blue), and imaged with an inverted fluorescent microscope. DAPI, 4,6-diamidino-2-phenylindole. Color images available online at www.liebertpub.com/tea

aggregates had $<20\,\mu m$ size in 2.5 and 5.3 kPa gels, respectively. Further, for the gel with 5.3 kPa modulus, 23% and 8% of 4T1 tumorspheres and 8% and 3% of MCF7 tumorspheres had size in the range of 80–120 and 120–200 μm, respectively. The fraction of tumorspheres with 0–20-μm diameter (single-cell fraction) increased with increasing gel modulus for 4T1 and MCF7 cells and all of the cells in the highest modulus gel (68.6 kPa) remained as single cells.

The number density of viable 4T1 and MCF7 cells in PEGDA gels with different moduli is shown in Figure 7C and 7F, respectively. The cell count increased with time for all groups but the gels with moduli of 2.5 and 5.3 kPa had the highest cell count at all time points. At each time point, the change in cell count with gel modulus was bimodal; that is, the cell count initially increased for moduli of 2.5 and 5.3 kPa and then decreased for gels with moduli >26 kPa. At day 14, the 5.3 kPa gel had 3-fold higher 4T1 cells and 1.3-fold higher MCF7 cells than the 2.5 kPa gel; the 5.3 kPa gel had 10-fold higher 4T1 and MCF7 cells than those gels with >26 kPa modulus. In general, the gel modulus has similar effects on 4T1 and MCF7 cells. These results demonstrated that the gel with modulus of 5.3 kPa had the highest potential for tumorsphere formation in the absence of ligand–receptor interactions.

Tumorsphere marker expression

One of the unique properties of CSCs is asymmetrical division and retention of DNA labeling.[37] Based on this feature, BrdU retention is a commonly used method to characterize CSCs. 4T1 cells were labeled with BrdU before encapsulation in the PEGDA gel with 5.3 kPa modulus and the intensity of BrdU staining was compared with those cells cultured on ultra-low-attachment plates. Figure 8 compares BrdU staining of 4T1 cells in suspension culture on ultra-low-attachment plates (Fig. 8A, C) with those encapsulated in PEGDA hydrogels (Fig. 8B, D). Images A and B in Figure 8 are after 8 days of culture while images C and D are after 14 days. After 8 and 14 days, cells encapsulated in the gel displayed higher level of BrdU retention than those in suspension cultures, suggesting that the encapsulated tumorspheres had higher fraction of CSCs.

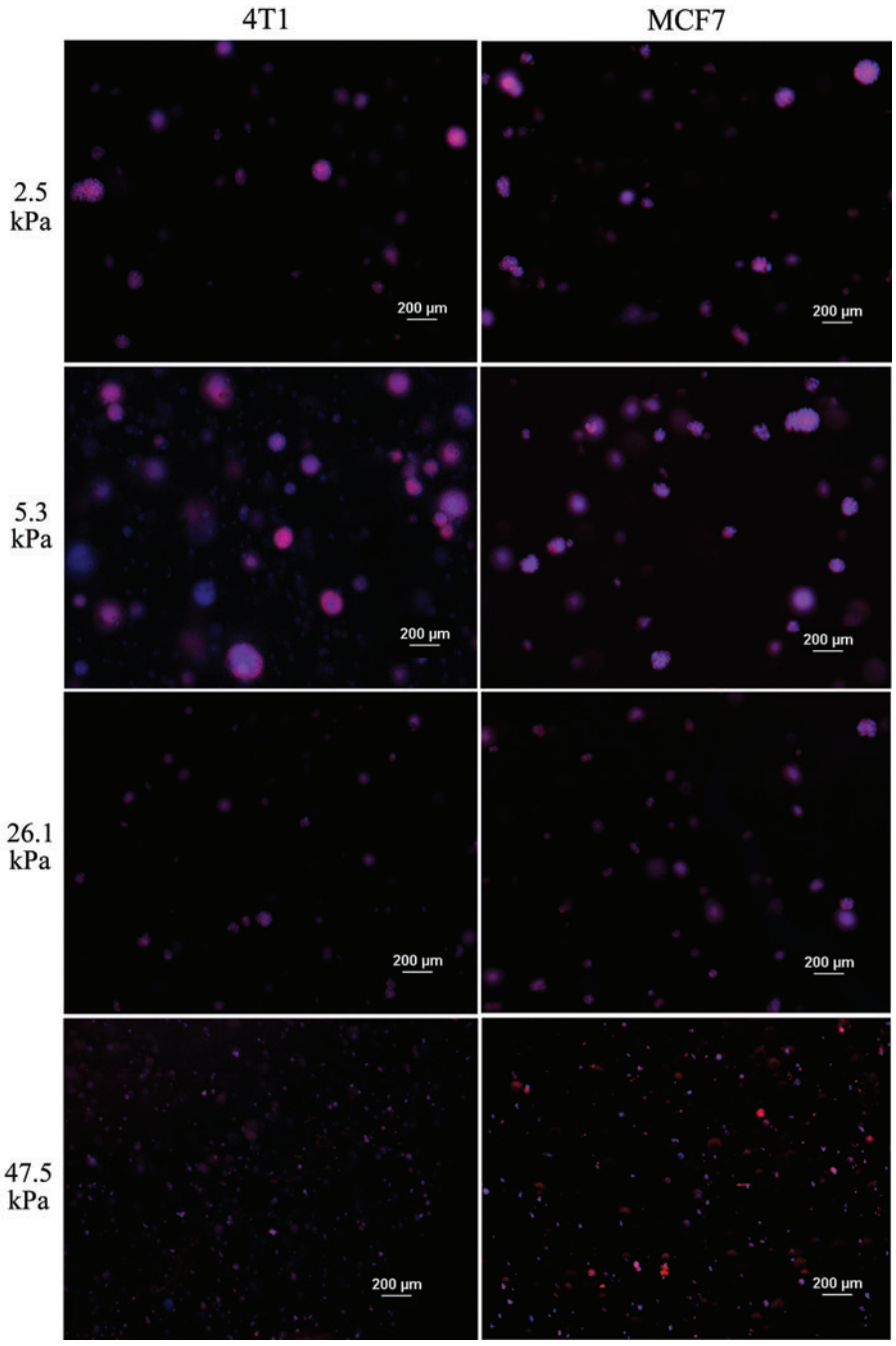

FIG. 6. Representative images of tumorsphere density for 4T1 (left column) and MCF7 (right column) cells encapsulated in PEGDA hydrogels with elastic modulus of (A) 2.5 kPa (first row), 5.3 kPa (second row), 26.1 kPa (third row), and 47.5 kPa (fourth row) after 8 days of incubation. At each time point, encapsulated cells were stained with phalloidin for cytoskeleton (red) and DAPI for nucleus (blue), and imaged with an inverted fluorescent microscope. Color images available online at www.liebertpub.com/tea

The expression of breast CSC markers for tumorspheres grown in PEGDA gels with different moduli is shown in Figure 9. Figure 9A–D shows the expression of CD44, CD24, ABCG2, and SCA1 for 4T1 cells and Figure 9E and 9F shows the expression of CD44 and ABCG2 for MCF7 cells. ABCG2 of ABC transporter proteins is responsible for CSC drug resistance and SCA1 (stem cell antigen-1) is a cell surface protein known to be associated with breast CSCs.[48–50] CD44 and ABCG2 are well-studied markers in both mouse and human breast CSCs.[51,52] Although CD24− is also a marker often used as a breast CSC marker, recent studies indicate that both CD44+/CD24− and CD44+/CD24+ cells display CSC phenotypes in MCF7 cells.[53] SCA1 is a murine stem cell marker and it is unclear whether SCA1 is a CSC marker in human cancer cells. In addition, the coding sequence of human SCA1 is not well defined. Therefore, only the expression of CD44 and ABCG2 markers was examined for MCF7 cells. 4T1 cells in the gel with elastic modulus of 5.3 kPa had the highest CD44 expression and lowest CD24 expression for all time points. CD44 expression of 4T1 and MCF7 cells initially increased and reached a maximum at day 8 for 2.5 and 5.3 kPa gels and at day 11 for 26.1 kPa gel. CD44 expression then decreased with incubation time. 4T1 and MCF7 cells encapsulated in the gels with moduli of 47.5 and 68.6 kPa did not show an increase in CD44 expression in 14 days. This biphasic marker expression with time was also observed for ABCG2 marker in 4T1 and MCF7 cells. At day 8, CD44 and ABCG2 expression of 4T1 cells increased by 2.2- and 1.8-fold,

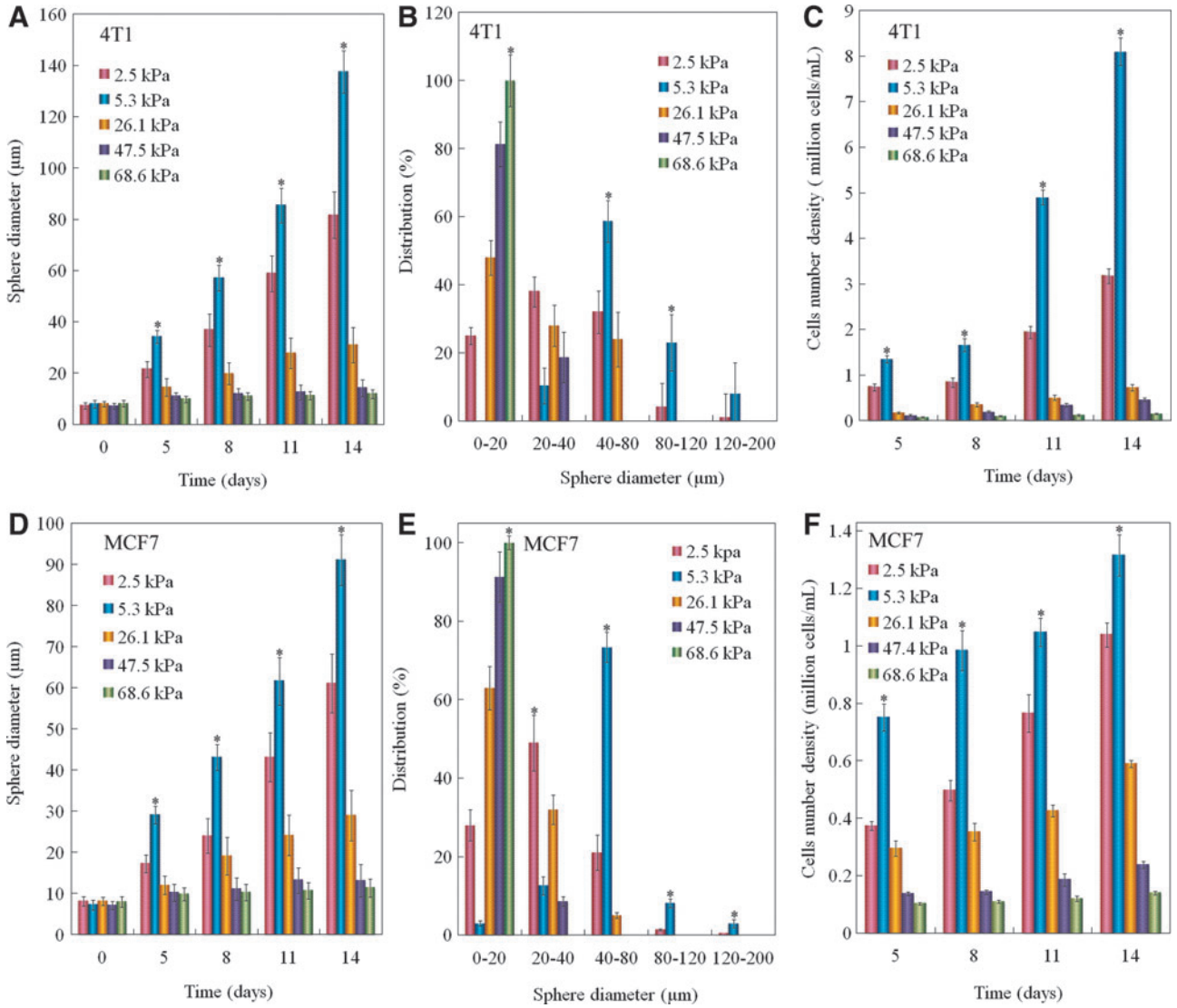

FIG. 7. Average tumorsphere size **(A, D)**, tumorsphere size distribution **(B, E)**, and cell count **(C, F)** for 4T1 and MCF7 tumor cells encapsulated in PEGDA hydrogels with different elastic moduli and incubated for up to 14 days. Graphs **(A–C)** and **(D–F)** correspond to 4T1 and MCF7 cells, respectively. The symbol asterisk indicates statistically significant difference between the test group and all other groups at the same time point **(A, C, D,** and **F)** or at the same tumorsphere diameter range **(B, E)**. Error bars correspond to mean ± 1 SD for $n = 3$. Color images available online at www.liebertpub.com/tea

respectively, with increase in gel modulus from 2.5 to 5.3 kPa; those for MCF7 cells increased by 1.2- and 1.7-fold with increase in gel modulus from 2.5 to 5.3 kPa.

To determine whether tumorspheres in the hydrogel had a higher level of stem cell population than those formed on ultra-low-attachment plates, CD44 immunostaining of the 4T1 cells encapsulated in PEGDA gels (5.3 kPa modulus) was compared with those cultured on ultra-low-attachment plates after 5, 8, and 11 days of culture, and the results are shown in Figure 10. Tumorspheres grown in the gel and on ultra-low-attachment plate both had high level of CD44 staining after 5 and 8 days of culture and the intensity of CD44 staining started to decrease after 8 days of culture for both groups. This was consistent with our CD44 mRNA data (see Fig. 9). However, tumorspheres grown in the gel had a more intensive CD44 staining than those on ultra-low-attachment plates for longer incubation times of 11 and 14 days, suggesting that the 3D microenvironment and gel stiffness modulated the maintenance of stemness in CSCs.

Discussion

The ECM stiffness regulates proliferation and differentiation of many cell types.[54–56] Development of solid tumors is often accompanied by an increase in the stiffness of the local environment. For example, high tissue density is a known risk factor for developing invasive breast carcinoma.[57,58] The stiffness of normal human breast tissue is lower than 4 kPa while that of cancerous breast tissue can be up to 40 kPa.[59] Analysis of several cell lines in collagen matrices has revealed that matrix stiffness can dramatically affect the growth of certain cell lines but has little effect on others.[60] For example, the growth of MDA-MB-231 cells, a highly malignant human breast cancer cell line, is significantly enhanced

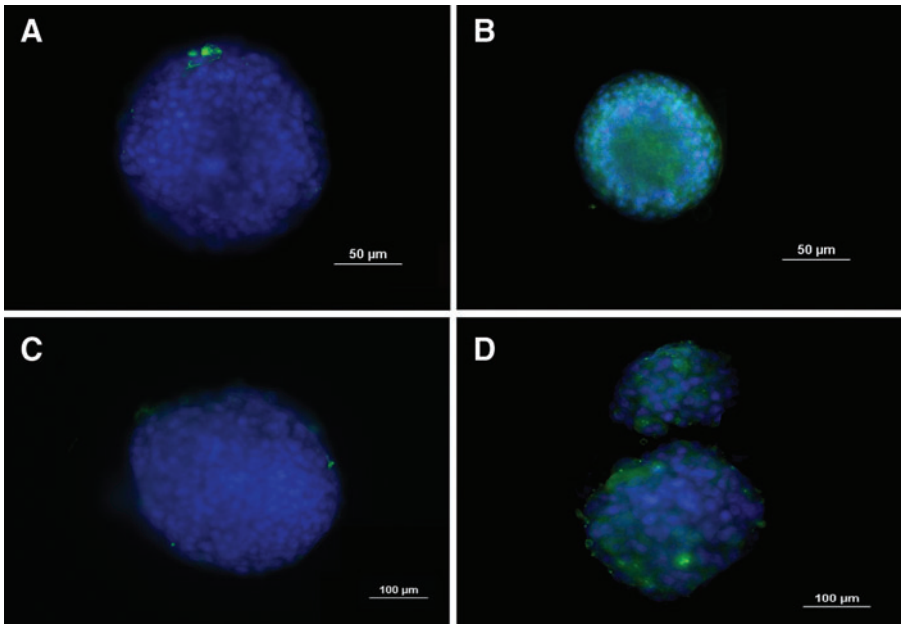

FIG. 8. BrdU staining of 4T1 tumorspheres formed in suspension culture on low-adhesion plates **(A, C)** and formed by encapsulation in PEGDA hydrogels **(B, D)**. Images **(A)** and **(B)** are after 8 days of incubation while images **(C)** and **(D)** are after 14 days. Prior to tumorsphere formation, 4T1 cells were incubated with BrdU for 10 days to achieve stable labeling. The presence of BrdU in the cells was confirmed by immunofluorescent staining (green). The cell nuclei were stained with DAPI (blue). BrdU, bromodeoxyuridine. Color images available online at www.liebertpub.com/tea

with increasing matrix stiffness while the growth of MCF-10a, a nonmalignant breast epithelial cell line, is relatively insensitive to matrix stiffness within a certain range.[60] These results suggest that the response of cancer cells to matrix stiffness is not only dependent on the cancer but also on malignancy of the cancer. Further, it has been reported that nontumorigenic breast epithelial cells loose cell polarity and increase proliferation when cultured in matrices with 4.5 kPa stiffness.[61] In addition, normal murine mammary gland or well-differentiated mammary epithelial cells cultured in high-density collagen matrices display an invasive phenotype.[62] Mechanistic studies suggest that these mechanically induced transformations are associated with enhanced focal adhesion kinase (FAK) followed by FAK-dependent ERK and Rho activity.[62,63] These pathways have been suggested as the circuit linking matrix stiffness to cytoskeleton.[62,63] PEGDA hydrogels used in this study do not have cell adhesion ligands that are believed to mediate mechanosensing.[26] The cell response to stiffness in the inert PEG matrix may be through the ECM secreted by the encapsulated tumor cells. For example, human mesenchymal stem cells (hMSCs) encapsulated in PEG hydrogels, in the absence of adhesive ligands, secret their own ECM through which differentiation is directed by mechanotransduction.[64]

According to rubber elasticity theory, the gel elastic modulus is proportional to the density of elastically active chains or crosslink density.[65] The network crosslink density increased with increasing acrylate concentration in PEGDA precursor solution, leading to the increase in matrix modulus. The range of elastic moduli selected in this study was based on the reported stiffness of breast tumor tissue.[59,66] Increasing evidence suggests that CSCs are responsible for tumor initiation and metastasis as well as drug resistance.[67] Maintenance of CSCs *in vivo* is highly dependent on the tumor microenvironment. Stem cell microenvironments *in vivo* are polarized structures with individual stem cells exposed to different niche components.[68,69] We have shown in this study that the formation of spheroids by 4T1 tumor cells encapsulated in an inert matrix is biphasic with respect to matrix modulus in the 2.5–68.6 kPa range. The initial increase in tumorsphere size and cell number density with elastic modulus may be attributed to a deviation from normal tissue stiffness ($\sim$0.17 kPa), leading to matrix reorganization and change in the number and lifetime of integrin-mediated interactions and related pathways.[26] It has been reported that the sphere size of breast cancer cells encapsulated in collagen gels increased with elastic modulus from 0.17 to 1.20 kPa.[61] In another study, it was shown that the proliferation and sphere size of hepatocellular carcinoma cells encapsulated in PEG–collagen gels increased with decreasing elastic modulus from 4 kPa (corresponding to the modulus of healthy liver) to 0.7 kPa.[70] A decrease in sphere size and cell number for gel moduli >5.3 kPa can be attributed to a decrease in mesh size and increase in retractive force of the gel network, leading to a negative contribution on the cell proliferation and sphere formation.[71] The average pore size or the mesh size of the hydrogel can affect diffusion of nutrients and oxygen and tumor cell motility. For example, HepG2 hepatocellular carcinoma cells form larger spheres when encapsulated in alginate gels with larger pore sizes.[72] The mesh size of the PEGDA gels was calculated from the modulus and equilibrium swelling ratio of the gels using the Peppas and Barr-Howell equation, as described.[73] As the macromer concentration was increased from 7.5% to 10%, 15%, 20%, and 25%, the mesh size decreased significantly from 93 ± 4 nm to 67 ± 3, 53 ± 3, 34 ± 2, and 25 ± 2 nm, respectively. Therefore, the bimodal effect of gel modulus on tumorsphere formation may be due to the changes in the network mesh size, as well as the gel modulus, that can affect cell–matrix interactions and nutrient diffusion.

The formation of tumorspheres is associated with breast CSC markers, suggesting that sphere formation in the gel matrix is not caused by simple cell aggregation but by CSCs. It has been shown that matrix stiffness can alter the expression of CSC markers in hepatocellular carcinoma cells encapsulated in a collagen matrix.[23] Unlike collagen and other

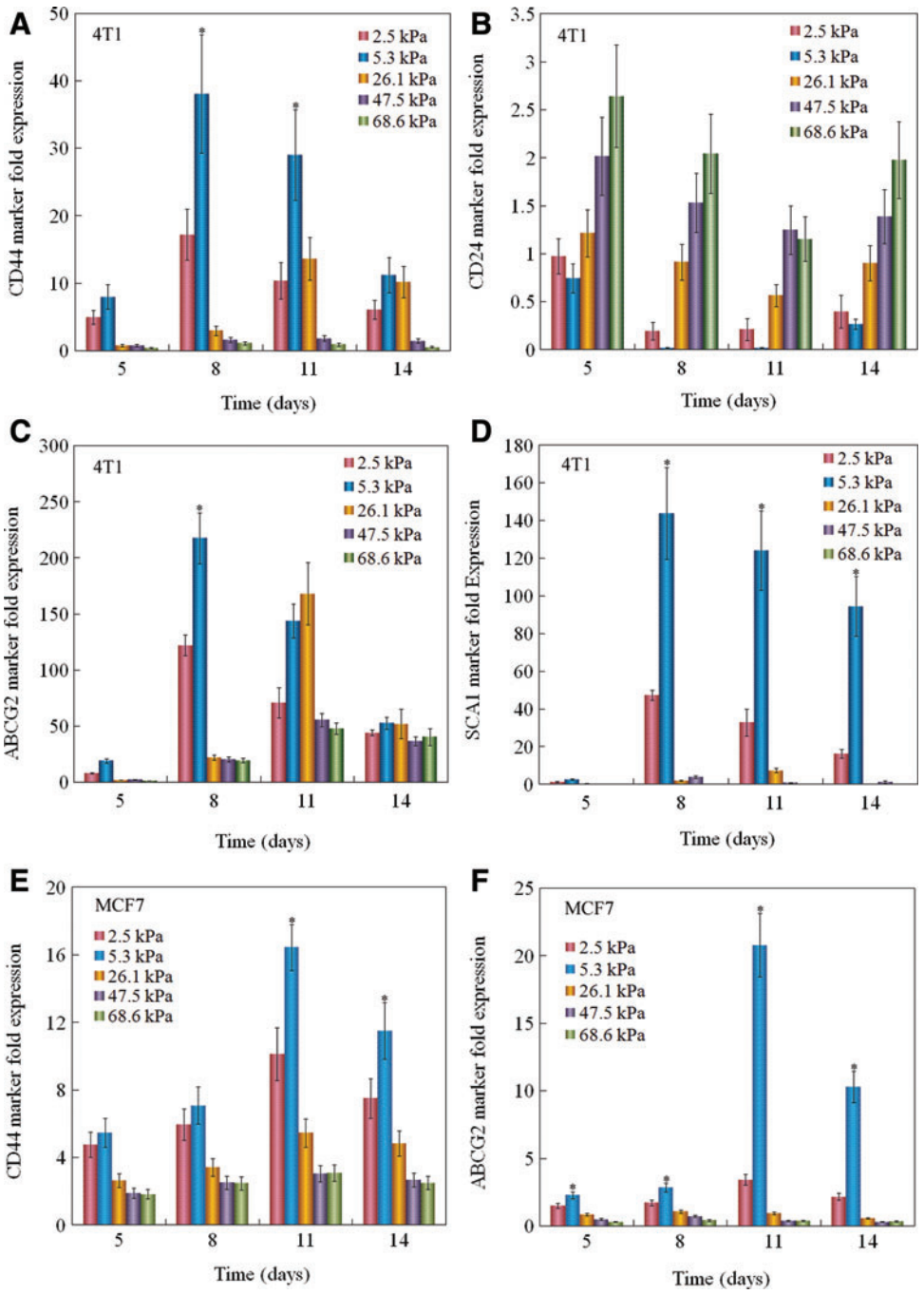

FIG. 9. Effect of gel elastic modulus on the relative mRNA expression levels of CD44 **(A)**, CD24 **(B)**, ABCG2 **(C)**, and SCA1 **(D)** markers of 4T1 cells, and CD44 **(E)** and ABCG2 **(F)** markers of MCF7 cells encapsulated in PEGDA hydrogels with incubation time. The mRNA expression levels of the markers for 4T1/MCF7 cells before encapsulation were used as reference (set equal to one). The symbol asterisk indicates statistically significant difference between the test group and all other groups at the same time point. Error bars correspond to mean ± 1 SD for $n = 3$. Color images available online at www.liebertpub.com/tea

biological gels, varying PEGDA macromer concentration only changes the gel stiffness, not the ligand density in the matrix. Our results suggest that the stiffness of the tumor tissue alone is sufficient to affect the fate of tumor cells. A biphasic behavior of CSC marker expression with time may be attributed to the fraction of CSCs in the gel. The CSC fraction initially increased with loss of normal tumor cells in the inert low-adhesive PEGDA gel. Then, the fraction started to decrease as the rate of differentiation of CSCs to normal cancer cells was higher than the rate of transformation of differentiated cells to CSCs.[74] The highest expression of CD44 and ABCG2 markers at day 8 and largest tumorsphere size for 4T1 and MCF7 cells encapsulated in the gel with 5.3 kPa modulus indicates the existence of highest fraction of stem-like subpopulation at this matrix modulus. The fraction of CSCs in a tumor also depends on the microenvironment.[67] The concentration of oxygen and nutrients in the center of large tumorspheres may be lower than that for small spheres, leading to the formation of a hypoxic condition in the central part of the spheres in the 5.3 kPa gel, which in turn can increase the expression of CSC markers.[67,75]

Naturally derived gels, such as alginate and agarose gels, have also been used to study the behavior of breast cancer cells under a 3D condition. For example, highly invasive rat mammary carcinoma MTLn3-Mena cells form tumorspheres when encapsulated into alginate hydrogels, and the

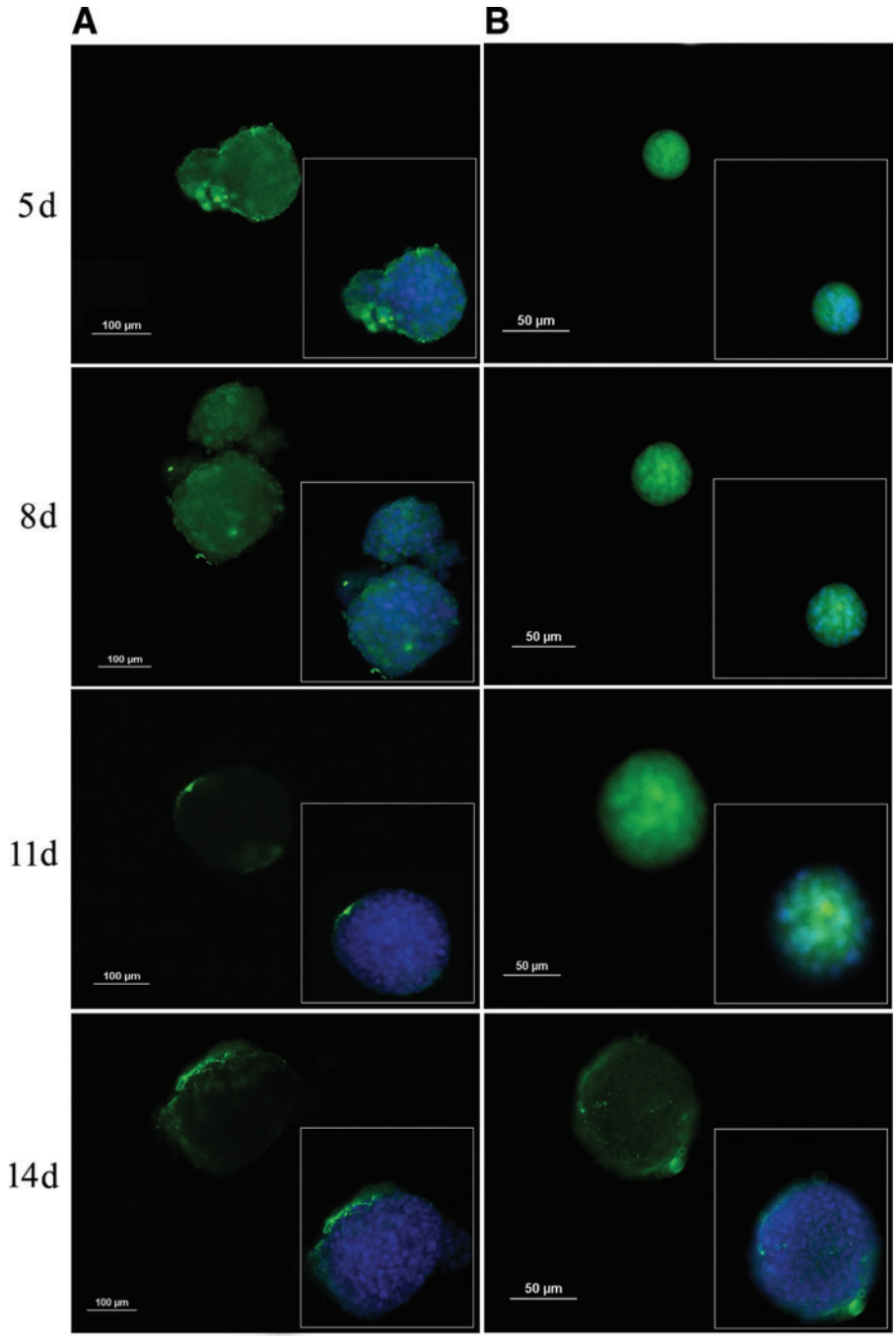

FIG. 10. Expression pattern of CD44 marker of 4T1 tumorspheres formed in suspension culture on low-adhesion plates **(**column **A)** and formed by encapsulation in PEGDA hydrogel with 5.3 kPa elastic modulus **(**column **B)**. Images in rows 1, 2, 3, and 4 are after 5, 8, 11, and 14 days of incubation, respectively. The cell nuclei were stained with DAPI (blue). Color images available online at www.liebertpub.com/tea

formation of tumorsphere can be inhibited by coculture with embryonic stem cells.[8] In another study, encapsulation of neoplastic cells in a growth-restricting hydrogel composed of agarose matrix leads to the selection of a stem cell subpopulation and the formation of tumorspheres.[9] However, our work demonstrates for the first time that CSCs can be maintained in the inert microenvironment of synthetic PEG hydrogels and the elastic modulus of the gel affects the growth of tumorspheres. The growth and maintenance of CSCs in other synthetic gels, such as polyhydroxyethyl methacrylate, polyvinylpolypyrrolidone, and polyvinyl alcohol, is of interest and will be investigated in future works.

Our results also show that 4T1 cells form higher number of tumorspheres when encapsulated in the PEG hydrogel compared with suspension cultures on low-adhesion plates. There are two possible explanations for this observation. One explanation is that the 3D hydrogel culture system more closely mimics the *in vivo* tissue environment than the suspension cultures with respect to the survival of CSCs. Evidence supporting this notion is that cancer cells have fewer number of CSCs in 2D cultures than the *in vivo*.[76] The elastic retractive force of the gel network can promote viability and proliferation of CSCs by enhancing FGF signaling and protein Kinase B (AKT) activation.[77,78] The other explanation is that the retractive force of the gel can induce the transformation of differentiated bulk cancer cells into CSCs. The transformation between CSCs and differentiated cancer cells is not unidirectional. Recent studies indicate that inducing

epithelial-to-mesenchymal transition (EMT) is sufficient to transform a differentiated cancer cell into a CSC.[79,80] In the process of EMT, tumor cells undergo cytoskeletal reorganization with subsequent changes in cell adhesion. At the molecular level, the key features of EMT include the altered expression of cell membrane proteins, such as E-cadherin and β-catenin, and cell polarity. It is known that mechanical properties as well as biochemical composition in the tumor microenvironment play profound roles in EMT.[81,82] It is possible that the hydrogel stiffness shifts the balance of EMT by regulating the conformation of cell membrane receptors and cell polarity. One example of such mechanism is epidermal growth factor receptor (EGFR) signaling that has been associated with breast CSC maintenance.[83] Compression of the cell membrane by the gel retractive force can shrink the interstitial space and increase the local ligand and receptor concentrations, thus increasing the autocrine EGFR signaling.[84]

Several signal transduction pathways, such as Notch, Wnt, and Hedgehog, have been identified to be critical for CSC maintenance.[85] It is unclear how these pathways are regulated by the matrix modulus as these pathways are normally activated by ligand binding to cell surface receptors, which was absent in PEGDA gels. A possible explanation is receptor clustering induced by compression of the cell by the elastic retractive force of the gel network. Future work should focus on the effect of gel modulus, in the absence of ligand–receptor interaction, on the expression and activity of the components of these pathways and how stiffness-modulated tumorsphere formation is altered when these pathways are blocked. It should be mentioned that the effect of matrix modulus on viability, growth, and differentiation of normal stem cells has been investigated. For example, the fate of MSCs encapsulated in alginate or agarose gels conjugated with cell-binding RGD peptides is regulated by the elastics modulus of the matrix. The encapsulated MSCs differentiated to the osteogenic lineage in the gel with an intermediate modulus (11–30 kPa) while they differentiated into the adipogenic lineage in the gel with a low modulus (2.5–5 kPa).[26] Similarly, MSCs encapsulated in PEG–silica gels with an intermediate elastic modulus (10–30 kPa) display edosteogenic phenotype.[86] It appears that matrix modulus affects the differentiation of normal stem cells while it affects maintenance and growth of tumorspheres in the case of CSCs.

In this work, the effect of matrix modulus on tumorsphere formation and maintenance of CSCs was investigated in an inert matrix without the interference of other factors. The PEG matrix can be used as a 3D model system to dissect the role of individual factors in the tumor microenvironment on tumorigenesis and maintenance of CSCs. For example, different types and concentration of ligands that interact with tumor cells can be conjugated to the PEGDA matrix without altering the physical and mechanical properties of the gel to study the effect of ligand–receptor interactions on CSC maintenance.

Conclusions

4T1 breast cancer cells were encapsulated in inert PEGDA hydrogels and the effect of gel modulus on tumorsphere formation and the expression of markers for CSCs were investigated. The gel modulus had a strong bimodal effect on tumorsphere formation and the expression of CSC markers. The gel elastic modulus ranged from 2.5 to 70 kPa. 4T1 cells encapsulated in the gel with modulus of 5.3 kPa had the highest growth rate and formed the largest and highest number of tumorspheres. Similar results were obtained when MCF7 human adenocarcinoma cell line was encapsulated in the PEGDA hydrogel. Tumorspheres formed by mouse 4T1 and human MCF7 cells encapsulated in the 5.3 kPa gel showed the highest expression of breast CSC markers CD44 and ABCG2 and the expression of CSC markers peaked after 8 days of incubation. For the first time in this work, the effect of matrix modulus on tumorsphere formation and maintenance of CSCs was investigated in an inert matrix without the interference of other factors. The inert PEG matrix can be used as a 3D model system to dissect the role of individual factors in the tumor microenvironment on tumorigenesis and maintenance of CSCs.

Acknowledgments

This work was supported by research grants to E. Jabbari from the National Science Foundation under grant Nos. CBET0756394, CBET0931998, and DMR1049381, and the National Institutes of Health under grant No. DE19180. The authors thank Mr. Danial Barati for assistance in synthesis of PEGDA macromer. E. Jabbari thanks Dr. Ralph A. Reisfeld (Scripps Research Institute) for providing the 4T1 murine breast carcinoma cells. The authors thank Dr. Jay Blanchette (Chemical Engineering at University of South Carolina) for the use and assistance with Nikon inverted fluorescent microscope.

Disclosure Statement

No competing financial interests exist.

References

1. Castano, Z., Tracy, K., and McAllister, S.S. The tumor macroenvironment and systemic regulation of breast cancer progression. Int J Dev Biol **55,** 889, 2011.
2. Haycock, J.W. 3D cell culture: a review of current approaches and techniques. Methods Mol Biol **695,** 1, 2011.
3. Petersen, O.W., Ronnov-Jessen, L., Howlett, A.R., and Bissell, M.J. Interaction with basement membrane serves to rapidly distinguish growth and differentiation pattern of normal and malignant human breast epithelial cells. Proc Natl Acad Sci U S A **89,** 9064, 1992.
4. Pampaloni, F., Reynaud, E.G., and Stelzer, E.H. The third dimension bridges the gap between cell culture and live tissue. Nat Rev Mol Cell Biol **8,** 839, 2007.
5. Debnath, J., and Brugge, J.S. Modelling glandular epithelial cancers in three-dimensional cultures. Nat Rev Cancer **5,** 675, 2005.
6. Dawson, E., Mapili, G., Erickson, K., Taqvi, S., and Roy, K. Biomaterials for stem cell differentiation. Adv Drug Deliv Rev **60,** 215, 2008.
7. Masters, K.S., Shah, D.N., Walker, G., Leinwand, L.A., and Anseth, K.S. Designing scaffolds for valvular interstitial cells: cell adhesion and function on naturally derived materials. J Biomed Mater Res A **71,** 172, 2004.
8. Raof, N.A., Raja, W.K., Castracane, J., and Xie, Y.B. Bioengineering embryonic stem cell microenvironments for exploring inhibitory effects on metastatic breast cancer cells. Biomaterials **32,** 4130, 2011.

9. Smith, B.H., Gazda, L.S., Conn, B.L., Jain, K., Asina, S., Levine, D.M., Parker, T.S., Laramore, M.A., Martis, P.C., Vinerean, H.V., David, E.M., Qiu, S.Z., Cordon-Cardo, C., Hall, R.D., Gordon, B.R., Diehl, C.H., Stenzel, K.H., and Rubin, A.L. Three-dimensional culture of mouse renal carcinoma cells in agarose macrobeads selects for a subpopulation of cells with cancer stem cell or cancer progenitor properties. Cancer Res **71,** 716, 2011.
10. Cushing, M.C., and Anseth, K.S. Materials science: hydrogel cell cultures. Science **316,** 1133, 2007.
11. Bryant, S.J., and Anseth, K.S. Hydrogel properties influence ECM production by chondrocytes photoencapsulated in poly(ethylene glycol) hydrogels. J Biomed Mater Res **59,** 63, 2002.
12. Sawhney, A.S., Pathak, C.P., and Hubbell, J.A. Interfacial photopolymerization of poly(ethylene glycol)-based hydrogels upon alginate-poly(L-lysine) microcapsules for enhanced biocompatibility. Biomaterials **14,** 1008, 1993.
13. Chirila, T.V., Constable, I.J., Crawford, G.J., Vijayasekaran, S., Thompson, D.E., Chen, Y.C., Fletcher, W.A., and Griffin, B.J. Poly(2-hydroxyethyl methacrylate) sponges as implant materials: *in vivo* and *in vitro* evaluation of cellular invasion. Biomaterials **14,** 26, 1993.
14. Buxton, A.N., Zhu, J., Marchant, R., West, J.L., Yoo, J.U., and Johnstone, B. Design and characterization of poly(ethylene glycol) photopolymerizable semi-interpenetrating networks for chondrogenesis of human mesenchymal stem cells. Tissue Eng **13,** 2549, 2007.
15. Papadopoulos, A., Bichara, D.A., Zhao, X., Ibusuki, S., Randolph, M.A., Anseth, K.S., and Yaremchuk, M.J. Injectable and photopolymerizable tissue-engineered auricular cartilage using poly(ethylene glycol) dimethacrylate copolymer hydrogels. Tissue Eng A **17,** 161, 2011.
16. Doroski, D.M., Levenston, M.E., and Temenoff, J.S. Cyclic tensile culture promotes fibroblastic differentiation of marrow stromal cells encapsulated in poly(ethylene glycol)-based hydrogels. Tissue Eng A **16,** 3457, 2010.
17. Elisseeff, J., McIntosh, W., Anseth, K., Riley, S., Ragan, P., and Langer, R. Photoencapsulation of chondrocytes in poly(ethylene oxide)-based semi-interpenetrating networks. J Biomed Mater Res **51,** 164, 2000.
18. Rehfeldt, F., Engler, A.J., Eckhardt, A., Ahmed, F., and Discher, D.E. Cell responses to the mechanochemical microenvironment—implications for regenerative medicine and drug delivery. Adv Drug Deliv Rev **59,** 1329, 2007.
19. Singhvi, R., Kumar, A., Lopez, G.P., Stephanopoulos, G.N., Wang, D.I., Whitesides, G.M., and Ingber, D.E. Engineering cell shape and function. Science **264,** 696, 1994.
20. Engler, A.J., Sweeney, H.L., Discher, D.E., and Schwarzbauer, J.E. Extracellular matrix elasticity directs stem cell differentiation. J Musculoskelet Neuronal Interact **7,** 335, 2007.
21. Chen, C.S., Mrksich, M., Huang, S., Whitesides, G.M., and Ingber, D.E. Geometric control of cell life and death. Science **276,** 1425, 1997.
22. Discher, D.E., Janmey, P., and Wang, Y.L. Tissue cells feel and respond to the stiffness of their substrate. Science **310,** 1139, 2005.
23. Schrader, J., Gordon-Walker, T.T., Aucott, R.L., van Deemter, M., Quaas, A., Walsh, S., Benten, D., Forbes, S.J., Wells, R.G., and Iredale, J.P. Matrix stiffness modulates proliferation, chemotherapeutic response, and dormancy in hepatocellular carcinoma cells. Hepatology **53,** 1192, 2011.
24. Zaman, M.H., Trapani, L.M., Siemeski, A., MacKellar, D., Gong, H.Y., Kamm, R.D., Wells, A., Lauffenburger, D.A., and Matsudaira, P. Migration of tumor cells in 3D matrices is governed by matrix stiffness along with cell-matrix adhesion and proteolysis. Proc Natl Acad Sci U S A **103,** 10889, 2006.
25. Verbridge, S.S., Chandler, E.M., and Fischbach, C. Tissue-engineered three-dimensional tumor models to study tumor angiogenesis. Tissue Eng A **16,** 2147, 2010.
26. Huebsch, N., Arany, P.R., Mao, A.S., Shvartsman, D., Ali, O.A., Bencherif, S.A., Rivera-Feliciano, J., and Mooney, D.J. Harnessing traction-mediated manipulation of the cell/matrix interface to control stem-cell fate. Nat Mater **9,** 518, 2010.
27. Liu, S.Q., Tian, Q.A., Hedrick, J.L., Hui, J.H.P., Ee, P.L.R., and Yang, Y.Y. Biomimetic hydrogels for chondrogenic differentiation of human mesenchymal stem cells to neocartilage. Biomaterials **31,** 7298, 2010.
28. Sun, Y., Chen, C.S., and Fu, J. Forcing stem cells to behave: a biophysical perspective of the cellular microenvironment. Annu Rev Biophys **41,** 519, 2012.
29. Keung, A.J., Kumar, S., and Schaffer, D.V. Presentation counts: microenvironmental regulation of stem cells by biophysical and material cues. Ann Rev Cell Dev Biol **26,** 533, 2010.
30. Arai, F., Hirao, A., Ohmura, M., Sato, H., Matsuoka, S., Takubo, K., Ito, K., Koh, G.Y., and Suda, T. Tie2/angiopoietin-1 signaling regulates hematopoietic stem cell quiescence in the bone marrow niche. Cell **118,** 149, 2004.
31. He, X., Zhang, L., and Li, L.H. Cellular and molecular regulation of hematopoietic and intestinal stem cell behavior. Ann N Y Acad Sci **1049,** 28, 2005.
32. Li, L., and Neaves, W.B. Stem cells and cancer stem cells. Cancer Res **66,** 6458, 2006.
33. Yu, F., Li, J., Chen, H., Fu, J., Ray, S., Huang, S., Zheng, H., and Ai, W. Kruppel-like factor 4 (KLF4) is required for maintenance of breast cancer stem cells and for cell migration and invasion. Oncogene **30,** 2161, 2011.
34. Krohn, A., Song, Y.H., Muehlberg, F., Droll, L., Beckmann, C., and Alt, E. CXCR4 receptor positive spheroid forming cells are responsible for tumor invasion *in vitro*. Cancer Lett **280,** 65, 2009.
35. Gupta, P.B., Onder, T.T., Jiang, G.Z., Tao, K., Kuperwasser, C., Weinberg, R.A., and Lander, E.S. Identification of selective inhibitors of cancer stem cells by high-throughput screening. Cell **138,** 645, 2009.
36. Liu, J.C., Deng, T., Lehal, R.S., Kim, J., and Zacksenhaus, E. Identification of tumorsphere- and tumor-initiating cells in HER2/Neu-induced mammary tumors. Cancer Res **67,** 8671, 2007.
37. Fillmore, C.M., and Kuperwasser, C. Human breast cancer cell lines contain stem-like cells that self-renew, give rise to phenotypically diverse progeny and survive chemotherapy. Breast Cancer Res **10,** R25, 2008.
38. Tao, K., Fang, M., Alroy, J., and Sahagian, G.G. Imagable 4T1 model for the study of late stage breast cancer. BMC Cancer **8,** 228, 2008.
39. He, X., and Jabbari, E. Material properties and cytocompatibility of injectable MMP degradable poly(lactide ethylene oxide fumarate) hydrogel as a carrier for marrow stromal cells. Biomacromolecules **8,** 780, 2007.
40. He, X., Yang, X.M., and Jabbari, E. Combined effect of osteopontin and BMP-2 derived peptides grafted to an adhesive hydrogel on osteogenic and vasculogenic differentiation of marrow stromal cells. Langmuir **28,** 5387, 2012.
41. Fernandez-Gonzalez, R., Illa-Bochaca, I., Shelton, D.N., Welm, B.E., Barcellos-Hoff, M.H., and Ortiz-de-Solorzano,

C. *In situ* analysis of cell populations: long-term label-retaining cells. Methods Mol Biol **621,** 1, 2010.
42. Woodward, W.A., Chen, M.S., Behbod, F., and Rosen, J.M. On mammary stem cells. J Cell Sci **118,** 3585, 2005.
43. Weiswald, L.B., Guinebretiere, J.M., Richon, S., Bellet, D., Saubamea, B., and Dangles-Marie, V. *In situ* protein expression in tumour spheres: development of an immunostaining protocol for confocal microscopy. BMC Cancer **10,** 106, 2010.
44. Schefe, J.H., Lehmann, K.E., Buschmann, I.R., Unger, T., and Funke-Kaiser, H. Quantitative real-time RT-PCR data analysis: current concepts and the novel "gene expression's CT difference" formula. J Mol Med (Berl) **84,** 901, 2006.
45. Livak, K.J., and Schmittgen, T.D. Analysis of relative gene expression data using real-time quantitative PCR and the 2 (-delta delta C(T)) method. Methods **25,** 402, 2001.
46. Moeinzadeh, S., Khorasani, S.N., Ma, J.Y., He, X., and Jabbari, E. Synthesis and gelation characteristics of photo-crosslinkable star poly (ethylene oxide-co-lactide-glycolide acrylate) macromonomers. Polymer **52,** 3887, 2011.
47. Silverstein, R.M., Bassler, G.C., and Morril, T.C. Spectrometric Identification of Organic Compounds. New York: John Wiley, 1991.
48. Britton, K.M., Eyre, R., Harvey, I.J., Stemke-Hale, K., Browell, D., Lennard, T.W., and Meeson, A.P. Breast cancer, side population cells and ABCG2 expression. Cancer Lett **323,** 97, 2012.
49. Grange, C., Lanzardo, S., Cavallo, F., Camussi, G., and Bussolati, B. Sca-1 identifies the tumor-initiating cells in mammary tumors of BALB-neuT transgenic mice. Neoplasia **10,** 1433, 2008.
50. Welm, B., Behbod, F., Goodell, M.A., and Rosen, J.M. Isolation and characterization of functional mammary gland stem cells. Cell Prolif **Suppl 1,** 17, 2003.
51. Badve, S., and Nakshatri, H. Breast-cancer stem cells-beyond semantics. Lancet Oncol **13,** e43, 2012.
52. Kai, K., Arima, Y., Kamiya, T., and Saya, H. Breast cancer stem cells. Breast Cancer **17,** 80, 2010.
53. Bhat-Nakshatri, P., Appaiah, H., Ballas, C., Pick-Franke, P., Goulet, R., Badve, S., Srour, E.F., and Nakshatri, H. SLUG/SNAI2 and tumor necrosis factor generate breast cells with CD44+/CD24-phenotype. BMC Cancer **10,** 411, 2010.
54. Flanagan, L.A., Ju, Y.E., Marg, B., Osterfield, M., and Janmey, P.A. Neurite branching on deformable substrates. Neuroreport **13,** 2411, 2002.
55. Engler, A.J., Sen, S., Sweeney, H.L., and Discher, D.E. Matrix elasticity directs stem cell lineage specification. Cell **126,** 677, 2006.
56. Engler, A.J., Carag-Krieger, C., Johnson, C.P., Raab, M., Tang, H.Y., Speicher, D.W., Sanger, J.W., Sanger, J.M., and Discher, D.E. Embryonic cardiomyocytes beat best on a matrix with heart-like elasticity: scar-like rigidity inhibits beating. J Cell Sci **121,** 3794, 2008.
57. Gill, J.K., Maskarinec, G., Pagano, I., and Kolonel, L.N. The association of mammographic density with ductal carcinoma *in situ* of the breast: the multiethnic cohort. Breast Cancer Res **8,** R30, 2006.
58. Habel, L.A., Dignam, J.J., Land, S.R., Salane, M., Capra, A.M., and Julian, T.B. Mammographic density and breast cancer after ductal carcinoma *in situ*. J Natl Cancer Inst **96,** 1467, 2004.
59. Samani, A., Zubovits, J., and Plewes, D. Elastic moduli of normal and pathological human breast tissues: an inversion-technique-based investigation of 169 samples. Phys Med Biol **52,** 1565, 2007.
60. Tilghman, R.W., Cowan, C.R., Mih, J.D., Koryakina, Y., Gioeli, D., Slack-Davis, J.K., Blackman, B.R., Tschumperlin, D.J., and Parsons, J.T. Matrix rigidity regulates cancer cell growth and cellular phenotype. PLoS One **5,** e12905, 2010.
61. Paszek, M.J., Zahir, N., Johnson, K.R., Lakins, J.N., Rozenberg, G.I., Gefen, A., Reinhart-King, C.A., Margulies, S.S., Dembo, M., Boettiger, D., Hammer, D.A., and Weaver, V.M. Tensional homeostasis and the malignant phenotype. Cancer Cell **8,** 241, 2005.
62. Provenzano, P.P., Inman, D.R., Eliceiri, K.W., and Keely, P.J. Matrix density-induced mechanoregulation of breast cell phenotype, signaling and gene expression through a FAK-ERK linkage. Oncogene **28,** 4326, 2009.
63. Levental, K.R., Yu, H., Kass, L., Lakins, J.N., Egeblad, M., Erler, J.T., Fong, S.F., Csiszar, K., Giaccia, A., Weninger, W., Yamauchi, M., Gasser, D.L., and Weaver, V.M. Matrix crosslinking forces tumor progression by enhancing integrin signaling. Cell **139,** 891, 2009.
64. Parekh, S.H., Chatterjee, K., Lin-Gibson, S., Moore, N.M., Cicerone, M.T., Young, M.F., and Simon, C.G. Modulus-driven differentiation of marrow stromal cells in 3D scaffolds that is independent of myosin-based cytoskeletal tension. Biomaterials **32,** 2256, 2011.
65. Aklonis, J.J., MacKnight, W.J., and Shen, M. Introduction to Polymer Viscoelasticity. New York: Wiley-Interscience, 1972.
66. Nemir, S., and West, J.L. Synthetic materials in the study of cell response to substrate rigidity. Ann Biomed Eng **38,** 2, 2010.
67. Heddleston, J.M., Li, Z., Lathia, J.D., Bao, S., Hjelmeland, A.B., and Rich, J.N. Hypoxia inducible factors in cancer stem cells. Br J Cancer **102,** 789, 2010.
68. Hsu, Y.C., and Fuchs, E. A family business: stem cell progeny join the niche to regulate homeostasis. Nat Rev Mol Cell Biol **13,** 103, 2012.
69. Korkaya, H., Liu, S., and Wicha, M.S. Breast cancer stem cells, cytokine networks, and the tumor microenvironment. J Clin Invest **121,** 3804, 2011.
70. Liang, Y., Jeong, J., DeVolder, R.J., Cha, C., Wang, F., Tong, Y.W., and Kong, H. A cell-instructive hydrogel to regulate malignancy of 3D tumor spheroids with matrix rigidity. Biomaterials **32,** 9308, 2011.
71. Lee, B.H., Li, B., and Guelcher, S.A. Gel microstructure regulates proliferation and differentiation of MC3T3-E1 cells encapsulated in alginate beads. Acta Biomaterialia **8,** 1693, 2012.
72. Leal-Egana, A., Dietrich-Braumann, U., Diaz-Cuenca, A., Nowicki, M., and Bader, A. Determination of pore size distribution at the cell-hydrogel interface. J Nanobiotechnology **9,** 24, 2011.
73. Peppas, M.A., and Barr-Howell, B.D. Characterization of the crosslinked structure of hydrogels. In: Peppas, N.A., ed. Hydrogel in Medicine and Pharmacy. Boca Raton: CRC Press, 1986, pp. 27–56.
74. Tang, P., Ma, Q.H., Tang, Z.N., Wang, K.F., and Jiang, J. Long-term sphere culture cannot maintain a high ratio of cancer stem cells: a mathematical model and experiment. PLoS One **6,** e25518, 2011.
75. Soeda, A., Park, M., Lee, D., Mintz, A., Androutsellis-Theotokis, A., McKay, R.D., Engh, J., Iwama, T., Kunisada, T., Kassam, A.B., Pollack, I.F., and Park, D.M. Hypoxia promotes expansion of the CD133-positive glioma stem cells through activation of HIF-1 alpha. Oncogene **28,** 3949, 2009.

76. Vargo-Gogola, T., and Rosen, J.M. Modelling breast cancer: one size does not fit all. Nat Rev Cancer **7,** 659, 2007.
77. Vincent, T.L., Hermansson, M.A., Hansen, U.N., Amis, A.A., and Saklatvala, J. Basic fibroblast growth factor mediates transduction of mechanical signals when articular cartilage is loaded. Arthritis Rheum **50,** 526, 2004.
78. Adam, R.M., Roth, J.A., Cheng, H.L., Rice, D.C., Khoury, J., Bauer, S.B., Peters, C.A., and Freeman, M.R. Signaling through PI3K/AKT mediates stretch and PDGF-BB-dependent DNA synthesis in bladder smooth muscle cells. J Urol **169,** 2388, 2003.
79. Biddle, A., and Mackenzie, I.C. Cancer stem cells and EMT in carcinoma. Cancer Metastasis Rev PMID: 22302111, 2012.
80. Rhim, A.D., Mirek, E.T., Aiello, N.M., Maitra, A., Bailey, J.M., McAllister, F., Reichert, M., Beatty, G.L., Rustgi, A.K., Vonderheide, R.H., Leach, S.D., and Stanger, B.Z. EMT and dissemination precede pancreatic tumor formation. Cell **148,** 349, 2012.
81. Zeisberg, M., and Neilson, E.G. Biomarkers for epithelial-mesenchymal transitions. J Clin Invest **119,** 1429, 2009.
82. Floor, S., van Staveren, W.C., Larsimont, D., Dumont, J.E., and Maenhaut, C. Cancer cells in epithelial-to-mesenchymal transition and tumor-propagating-cancer stem cells: distinct, overlapping or same populations. Oncogene **30,** 4609, 2011.
83. Del Vecchio, C.A., Jensen, K.C., Nitta, R.T., Shain, A.H., Giacomini, C.P., and Wong, A.J. Epidermal growth factor receptor variant III contributes to cancer stem cell phenotypes in invasive breast carcinoma. Cancer Res **72,** 2657, 2012.
84. Tschumperlin, D.J., Dai, G., Maly, I.V., Kikuchi, T., Laiho, L.H., McVittie, A.K., Haley, K.J., Lilly, C.M., So, P.T., Lauffenburger, D.A., Kamm, R.D., and Drazen, J.M. Mechanotransduction through growth-factor shedding into the extracellular space. Nature **429,** 83, 2004.
85. Katoh, M. Networking of WNT, FGF, Notch, BMP, and Hedgehog signaling pathways during carcinogenesis. Stem Cell Rev **3,** 30, 2007.
86. Pek, Y.S., Wan, A.C.A., and Ying, J.Y. The effect of matrix stiffness on mesenchymal stem cell differentiation in a 3D thixotropic gel. Biomaterials **31,** 385, 2010.

Address correspondence to:
Esmaiel Jabbari, PhD
Associate Professor of Chemical and Biomedical Engineering
University of South Carolina
Swearingen Engineering Center, Rm 2C11
Columbia, SC 29208

E-mail: jabbari@engr.sc.edu

Received: May 31, 2012
Accepted: September 25, 2012
Online Publication Date: November 5, 2012